WARSAW UNIVERSITY OF TECHNOLOGY Index 351733
FACULTY OF CIVIL ENGINEERING
COMMITTEE FOR CIVIL AND WATER ENGINEERING
POLISH ACADEMY OF SCIENCES ISSN 1230-2945

DOI: 10.24425/ace.2020.136469

ARCHIVES OF CIVIL ENGINEERING

Vol. LXVII ISSUE 1 2021

EFFECT OF THE GROUND GRANULATED BLAST FURNACESLAG ON THE PORE STRUCTURE OF CONCRETE

ABDUL CHALID[1]

The objective of this study is to analyze effect of ground granulated blast furnace slag (GGBFS) in concrete on the pore structure, this research will contribute to the knowledge regarding the use of GGBFS as a cementitious material in terms of the future reference and potential improvement to the properties of concrete. To this aim, on the one hand a control specimens (CS) and another samples with 40% and 60% of GGBFS as replacement cement with moist cured at 20ºC, 27ºC, and cured at site. The compressive strength and the Mercury intrusion porosimetry (MIP) test were done. The result indicates that the strength of concrete with GGBFS at early ages tend to be lower in comparison with the CS. However, the GGBFS reaction plays important roles at the later ages. The samples cured at higher temperature produce higher strength value. The total pore volume (TPV) of the concrete use GGBFS decreases with increasing age.

Keywords: compressive strength, pore structure, GGBFS, cured at site, mercury intrusion porosimetry

[1] Senior Lectures Post Graduate of Civil Eng. Sangga Buana University, Jalan Surapati No. 189 Bandung-West Java 40123, Indonesia, e-mail: khaleedtu@yahoo.com

1. INTRODUCTION

GGBFS is an industrial byproduct that is widely used as ordinary Portland cement (OPC) replacement, and several extant studies focused on the same [1].The benefits of GGBF slag (when used as a partial replacement in cement) include the enhancement of long-term strength and durability of concrete, cost reduction, and a will be eco-friendly and economical [2]. In addition, the heat evolution was reduced when the replacement of GGBF slag was increased [3]. Due to blended of Portland cement (PC) and Ground Granulated Blast Furnace Slag (GGBFS) contains more silica and less than PC alone. The resulting microstructure of the hydrated cement past is densed. However, the initial hydration of GGBFS is very slow because it depends upon the breakdown of the glass by the hydroxyl ions released during the hydration on the PC. In a manner similar to blended cement containing pozzolans, reaction of GGBFS with calcium hydroxide take place [4]

MIP is a powerful technique which can be used to explore the structure of pores larger than about 3.5 nm. In the MIP, the volume of liquid metal that penetrates a solid is measured as a function of applied pressure. Subsequent analysis is based on the capillary law governing liquid penetration into small pores. Since mercury is a non-wetting liquid for most materials (its contact angle is greater than 90°), an externally imposed pressure is required to force it into the pores of a porous solid. The contact angle between mercury and concrete is only 117º, according to the [5], method, with which we determine more smaller the pore size, more greater the pressure required to force the mercury into the pore. In general, penetration data are analyzed using the Washburn equation [6]. These equations are generally accepted as a practical method of analyzing what are normally very complex pore systems

To determine the volume within any chosen range of pore sizes, the cumulative intruded pore volume vs log pore radius cure is plotted. In order to obtain a better understanding of the pore structure the cumulative distribution should be accompanied by the first differential distribution of the pore volume versus the pore radii. Therefore, a numerical fit of the cumulative distribution data using overlapping logarithmic curves was carried out. Each section of the fit was differentiated logarithmically in order to get the ordinate of the differential distribution.

A derivative distribution curve, consisting of dV/dlog R vs log pore radius, illustrates the rate of increase of intruded volume with increasing pore size. Hence, it is a measure of the relative frequency of occurrence of pores at any radius, down to 19 Å. The most common pore sizes are indicated by the

peaks of this curve. Typical curves that illustrate the appropriate effects will be presented. The effects of age, curing temperature and variation in replacement levels on OPC/GGBFS concrete were analyzed. The term large, medium and small pore size peak refer to peaks lying between 2000 to 5000 Å, 100 to 950 Å and 20 to 95 Å pore radii respectively

2. SPECIMEN PREPARATION AND TEST METHOD

2.1 CONCRETE SAMPLES

The mix proportions comprising of cement, GGBFS, coarse aggregate, fine aggregate and water for each batch of casting are shown in Table. The Table shows the total weight of mix proportion for 1 m^3 of concrete. [7] replaced up to 80% of cement by GGBFS making different substitutions. The good results were obtained in the substitutions up to 60%, since compressive strengths similar to conventional concrete were obtained. This study uses slag 40% and 60% as a substitute for cement for the optimum compressive strength test related to concrete porosity

Table 1. Mix Proportion of Concrete Containing GGBFS

Types	W/B	Cement (Kg)	GGBFS (Kg)	Water (Kg)	Fine Aggregate (Kg)	Coarse Aggregate (Kg)	Water Curing Temp.(°C)
Slag – 0 %	0.4	525	0	210	670	1,005	27 & Site
Slag – 40 %	0.4	315	210	210	670	1,005	20, 27, Site
Slag – 60 %	0.4	210	315	210	670	1,005	20, 27, Site

Table 2. Average of Physical Properties and Chemical Analysis of Cementitious Materials

Description Test	Portland Cement	GGBFS	Description Test	Portland Cement	GGBFS
Specific gravity (t/m^3)	3.28	2.90	Magnesium oxide (MgO)	2.60	4.60
Surface Area (m^2/kg)	314	420	Sulphur trioxide (SO_3)	1.80	2.20
Silica dioxide (S_iO_2)	20.20	28.2	Sodium oxide (Na_2O)	0.16	0.14
Aluminium oxide (Al_2O_3)	5.70	10.0	Potassium oxide (K_2O)	0.87	0.6
Ferric oxide (Fe_2O_3)	3	1.8	Loss on Ignition (LOI)*	2.7	0.2
Calcium oxide (CaO)	62.58	50.4	*This consist of moisture and CO2. High values are often an indication of poorly stored cement		

2.1.1 COMPRESSIVE STRENGTH TEST SAMPLES

100 mm cube specimens were casted in steel moulds. Placed was done in two layers, with each layer compacted by hand for 25 drops. Immediately after compaction, the excess concrete was removed and the top surface was levelled and smoothed using a trowel. The specimens were demoulded after 24 hours and marked for later identification followed by immediate curing in water at 20°C and 27°C.

The specimens with 100 x 210 x 2400 mm beam were casted in timber formwork. Casting was conducted at outside of the laboratory. The temperature ranged from 29 to 33°C, while the relative humidity stayed between 60 and 80%. The formworks were half-filled with concrete mix and compacted using a poker vibrator for three minute and covered by polythene. After 24 hours the sample demoulded and exposed to air at site. Samples curing used the burlap is moistened every day for one week. The specimens were cut into 100 mm cube size using concrete cutter before being tested.

2.1.2 MERCURY INTRUSION POROSIMETRY TEST SAMPLES

The remnants of compressive test specimens were crushed and the mortar portion was collected and dried in jars placed at room temperature. Finally, the samples were dried in the oven at 105ºC to remove any residual pore fluid. The oven drying took place for 3 days for achieving constant weight. The samples taken out from the oven and left to cool down before they were packed into polythene zip-lip bags and labelled for later identification.

2.2 MERCURY INTRUSION POROSIMETRY (MIP) TEST

An autoscan-60 porosimeter manufactured by Quanta chrome, USA was used throughout this investigation. The device is capable og generating pressures to a maximum value of 413 MN/m^2 (60.000 psi). The machine is the type that increases the mercury pressure in a continuous ram instead of the stepwise incremental pressure employed in a conventional porosimeter. This has the advantage of eliminating errors in both the pressure and volume readings caused by creep effect of the system components.

2.3 COMPRESSION TEST

Compression tests were performed using TONIPACT 3000 testing machine operating at a constant loading reate of 2–4 kN/sec. The samples which were cured in water were removed from the container and covered with wet tissue cover to retain the moisture before testing. The ends were dried and placed in the testing machine at room temperature in saturated state.

3. RESULT AND DISCUSSION

3.1 COMPRESSIVE STRENGTH

The Fig. 1 shows that at 3,7 and 28 days, the highest strength is obtained by CS, after 28 days specimens with 40% GGBFS achieve the highest strength. The Fig. 2 specimens cured at site at 180

days and 1 year show that the highest strength is given by sample incorporating 40% GGBFS, the lowest strength is 60% GGBFS of concrete. The strength of concrete using GGBFS at early ages within 28 days tend to be lower in comparison with the CS, particularly at higher replacement levels of GGBFS, because it depends upon the breakdown and dissolution of the glassy slag structure by

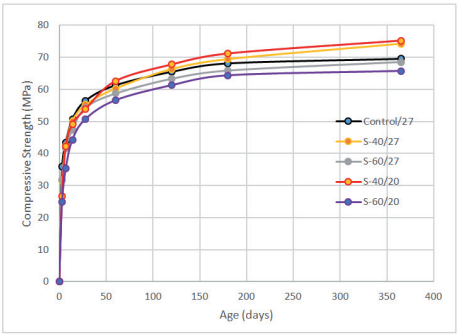

Fig. 1. The Compressive Strength of Concrete Containing GGBFS Moist Cured at 27ºC

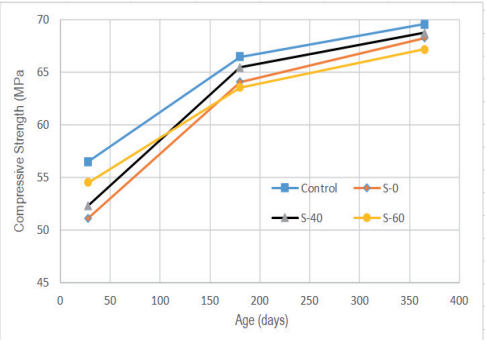

Fig. 2. The Compressive Strength of Concrete Containing GGBFS Moist Cured at Site

hydroxyl ions released during the hydration of OPC and also the alkali content in cement. The results of compressive strength also indicated that the GGBF slag content and particle size play important roles in the slag reaction at the later ages, whereas cement hydration is more prominent at the early ages [8]. The hydration of GGBFS consumes calcium hydroxide and uses it for additional Calcium-Silicate-Hydrate (CSH) formation, at same time, the GGBFS samples with cured at higher temperature produce higher strength value. The reactivity increases with fineness and since cement is more reactive than slag, reactivity also increases with decreasing replacement levels. Other factors that contribute to reactivity include chemical composition, hydration temperature, characteristics of the activator, water to cementitious ratio (W/B), and glass content. The Chemical composition, namely CaO, SiO2, Al2O3, MgO, and the overall hydraulic index (HI) were found to affect slag reactivity. Thirteen different proposed hydraulic indices, or hydraulic moduli, categorized into three different types are reviewed in [9]. There is relationship between the HI of slag at these ages and the influencing properties of slag [10-13].

3.2 THE CUMULATIVE INTRUDED PORE VOLUME VS LOG. PORE RADIUS

To determine the volume within any chosen range of pore sizes, the cumulative intruded pore volume vs log pore radius curve is plotted. In order to obtain a better understanding of the pore structure the

cumulative distribution should be accompanied by the first differential distribution of the pore volume versus the pore radii. Therefore, a numerical fit of the cumulative distribution data using overlapping logarithmic curves was carried out. Each section of the fit was differentiated logarithmically in order to get the ordinate of the differential distribution.

For the purpose of a qualitative comparison between cumulative distributions. Total intruded pore volume (mercury porosity) parameter will be identified to characterize the different distribution of pores. These parameter studies highlight the effect of age, GGBFS percentage, and curing temperature on the large pores within plain concrete and concrete incorporating GGBFS.

3.3 THE VARYING REPLACEMENT LEVEL OF GGBFS MOIST CURED AT 20ºC AND 27ºC

The pore size distribution and total porosity of the CC cured at 27ºC and cured in site are shown in Fig. 3-4. It can be seen that the CC at 28 days shows higher total porosity than the control specimen at 180 days. The lowest total porosity value is for specimen at 1 year. It clearly indicates that the TPV decreases with increasing age. The results also show the cumulative pore volume curves show distinct " knees" at medium pore radii in the curves. In generally the dV/dlog R curves for control concrete at 28, 180, and 1 year show predominantly single peak. The result also the "knees" at medium pore radii contain a large volume of pores as shown by the peaks occurring at the pore radii.

There is no significant shift in the positions of the peak observed with age of concrete. All specimens produce peaks al medium pore radii with broad base peak at between approximately 100 and 600 Å. It is seen that with increasing age, the height of the peak and the areas beneath are reduced. The curves have predominantly single peak. It lies at medium size pore radii in the region of approximately 300A. The height of the peak of medium pore radii is reduced whereas the peaks of small pore radii is enlarged with increased the height of peaks corresponding to increasing age. All specimens, the height of the peak lie at medium pore radii with broad base at between approximately 70Å and 700 Å. It can be seen that with increasing age, the height of the peak and areas beneath are reduced. [14] also reported that the total porosity increased with increasing GGBFS ratio in the specimens at early ages, whereas it decreased at later ages.

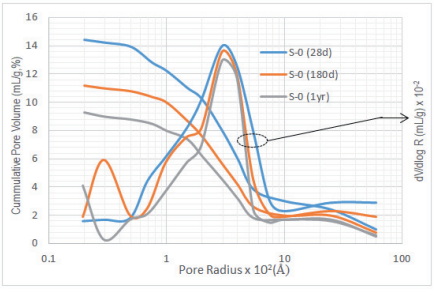

Fig. 3 Pore size and derivative distribution of Control Concrete moist cured at 27ºC

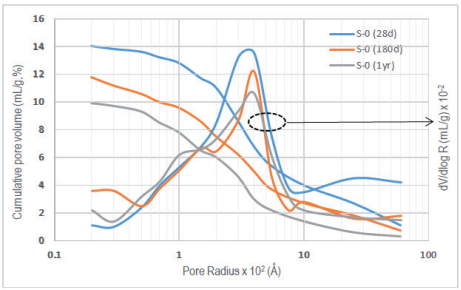

Fig. 4. Pore size and derivative distribution of plain concrete cored at site

Fig. 5-6 shows the TPV for concrete containing 40% GGBFS moist cured at 20ºC and 27ºC. The specimen at 1 year is lower in total porosity value than the concrete at 180 and 28 days. It clearly indicates that the TPV decreases with increasing age, however. these are not linearly. The Fig.5 shows that although there is significant change in TPV for specimen with increasing specimen age. There is no significant change in the derivative distribution for all specimen age. The curves have predominantly single peak. It lies at medium size pore radii in the region of approximately 400A.

Fig. 6. also shows that the significant change in TPV is followed by a significant change in derivative distribution of concrete at 28 days in comparison with the specimens at 180, and 1 year. The specimen has predominantly single peak. It lies at medium pore radii in the region at approximately 300Å. The specimens at 180 days and 1 year indicate that with increasing age the height of peaks and the areas beneath are changed The height of the peak of medium pore radii is reduced whereas the peaks of small pore radii is enlarged with the increasing the height of peaks corresponding to increasing age.

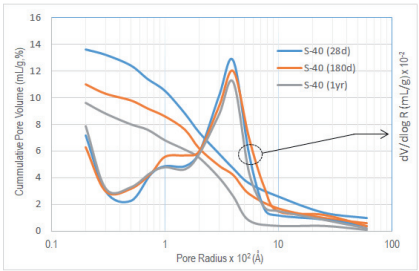

Fig. 5 Pore size and derivative distribution of Concrete for 40% GGBFS moist cured at 20ºC

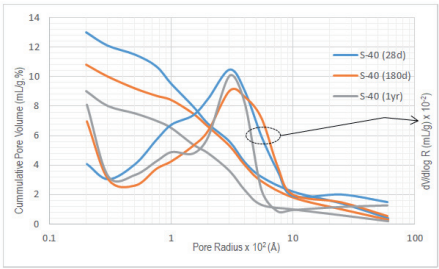

Fig. 6 Pore size and derivative distribution of Concrete for 40% GGBFS moist cured at 27ºC

Fig. 7-8 shows the TPV for specimen at 1 year produces the lowest than others. It clearly indicates the TPV decreases with increasing age. There is significant effects of age and cured temperature upon the size and shape of derivative distribution of the concrete containing 60% GGBFS cured at 20ºC

and 27ºC. It can be seen the samples at 28 days has predominantly single peaks. It lies at the medium size pore radii region at approximately 400 Å pore radii with increasing age the height of the peaks and the areas beneath are reduced. The results also show that the specimens at 180 days and 1 year are reduced in size of the peak at medium pore radii and shifted in position toward finer pore radii region. At the sometime it is observed, the peak at the small pore radii is enlarged with increased in the height of peaks. The Fig. 8 shows there is significant effects of age on the derivative distribution curves. At 28 days indicates the presence of predominantly single peak. It lies at medium size pore radii in the region with broad base at approximately 50 Å to 1000 Å pore radii. With increasing age, the height of the peaks and the areas beneath are reduced. The results also show the size and shape of these peaks are reduced and shifted in position toward finer pore radii region with enlarged pore radii

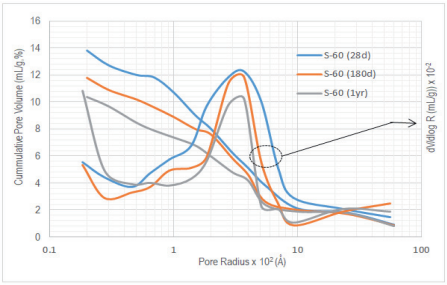

Fig. 7 Pore size and derivative distribution of Concrete for 60% GGBFS moist cured at 20ºC

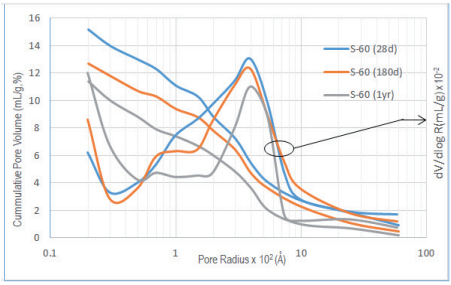

Fig. 8. Pore size and derivative distribution of concrete for 60% GGBFS moist cored at 27ºC

Fig. 9-10 shows TPV of concrete containing 40% and 60% GGBFS moist cured at site. Specimen at 1 year age produces the lowest total pore volume. This is followed by the concrete at 180 days, and 28 days. It can be seen that cumulative pore volume of 40% GGBFS at 180 days and 1 year has almost same value. The specimen cured at site after 28 days is in a relatively quick-hydrated process. It also clears from the above that the TPV decreases with increasing age, the dV/dLog R has broad base at small and medium pore radii regions and emerged at approximately 30 Å to 300Å pore radii. With increasing age the size and the position of these peaks are altered until many peaks remain. There is significant change in the size and position of these peaks with increasing age and the height of peak shifted in position toward finer pore radii region. The Figure also indicates with increasing age the height of the peaks shifted position toward finer pore radii region with enlarged peak. These results of this study contradict that reported by [15] confirmed that the peaks of the pore volume moved in the direction of the larger pore size due to the carbonation. In other studies, a shift in pore size of this tendency was observed, but the reason was considered to be the low amount of CH generation [16].

The reason for the shift of the pore peak of the specimens cured site towards a larger pore size compared with the peak of the moist cured remains unknown. Although verification is necessary, it is possible that the contraction caused by GGBFS may be the reason.

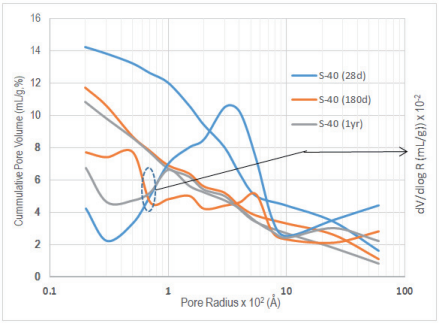

Fig. 9 Pore size and derivative distribution of concrete for 40% GGBFS moist cured at site

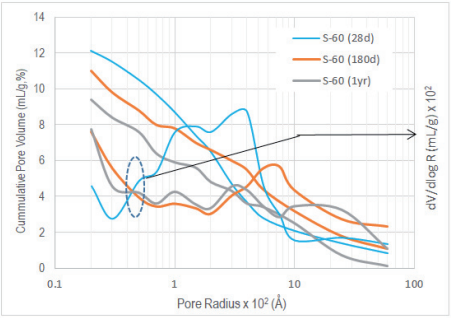

Fig. 10 Pore size and derivative distribution of concrete for 60% GGBFS moist cured at site

3.4 RELATIONSHIP BETWEEN PROPERTIES ENGINEERING AND PASTE PORE STRUCTURE OF CONCRETE

Replacement levels of GGBFS in the concrete moist cured at 27°C are show di Fig. 11. At 28 days control specimen achieves the highest total TPV. At 1 year, the highest cumulative pore volume is given by specimen for 60% GGBFS. This is followed by the control concrete. The optimum replacement levels of GGBFS is about 40% (based on 1 year total porosity results). Many researchers [14,17] found out there is relationship between engineering properties such as compressive strength and pore microstructure in concrete. Many equations [18] were established. However, these are depend essentially on the chemical and mineralogical composition of the clinker, W/B, curing temperature and conditions and consequently lead of different engineering properties.

The graph in Fig. 12 obtained from the compressive strength and total porosity values of the specimen at 28, 180, and 1 year. From the curve it is clear that, when the number of pore radii increased, the compressive strength and total porosity decreased or vice versa. [19,20] have reported that formation of low density product also improve strength because of an inherent reduction in porosity relative in high density products. Furthermore, at later ages, the GGBF slag produced a cementitious material that improved pore filling [21], created a denser microstructure, and enhanced the compressive strength obtained from the slag reaction when the GGBF slag replacement was increased.

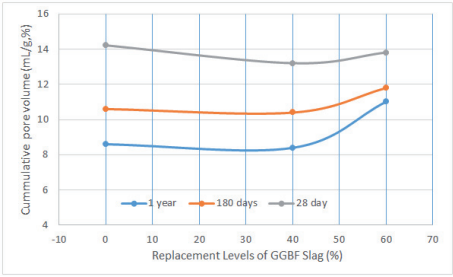

Fig. 11. Replacement level of GGBFS in concrete Moist cured at 27ºC

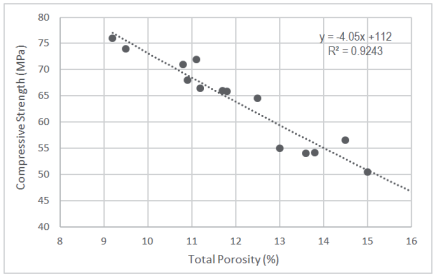

Fig. 12. Effect of compressive strength on total porosity value of concrete moist cured at 20ºC and 27ºC

4. CONCLUSION

The result indicates that the strength of concrete incorporating GGBFS at early ages tends to be lower in comparison with the control specimen, the results also show that the samples cured at higher temperature produce higher strength value. The results also indicate that systems with both supplementary materials had lower early strengths than pure cement, but could generally surpass pure cement paste after 90 days; higher slag content was particularly helpful for boosting the late strengths, it is comparable with have done.

The TPV of the concrete with replacement level of GGBFS decreases with increasing age. The dV/dLog R with GGBFS show that with increasing age, the height of the peaks and the areas beneath are reduced and shifted in position toward finer pore radii with enlarged pore radii or emerged the height of the peaks. For CC, there is no significant change of pore volume at later age, the most of pore radii lie at medium pore radii. The specimens cured at different curing temperature, the TPV of concrete using GGBFS is comparable with control specimens. Based on the specimens at 1 year total porosity results, the optimum replacement level of GGBFS is about 40%.

REFERENCES

1. Crossin, E. The greenhouse gas implications of using ground granulated blast furnace slag as a cement substitute. J. Clean. Prod. 95: 101–108, 2015
2. P Saranya*, Praveen Nagarajan, A P Shashikala," Eco-friendly GGBS Concrete: A State-of-The-Art Review," IOP Conf. Series: Materials Science and Engineering 330, 2018
3. H. A. Abola, C. K. King' Ondu, K. N. Njan, and A. L. Mrema, "Measurement of pozzolanic activity index of scoria, pumice, and rice hush ash as potential supplementary cementitious materials for Portland cement," Advances in Civil Engineering, vol. 2017, Article ID 6952645, 13 pages, 2017.
4. Neville, A, M.," Properties of Concrete', Fifth Edition, Pearson Education Limited Edinburgh Gate Harlow Essex CM20 2JE England, 2011
5. Kumar, R., & Bhattacharjee, B."Porosity, pore size distribution and in situ strength of concrete. Cement and Concrete Research, 33(1), 155-164, 2003

6. Washburn, E. W.,"The Dynamics of Capillary Flow". Physical Review. **17** (3): 273, 1921
7. Khatib J., Hibbert J., Khatib J. Selected engineering properties of concrete incorporating slag and metakaolin. Constr.Build.Mater.19:460–472, 2005
8. Punnaman Norrarat, Weerachart Tangchirapat, Smith Songpiriyakij, and Chai Jaturapitakkul," Evaluation of Strengths from Cement Hydration and Slag Reaction of Mortars Containing High Volume of Ground River Sand and GGBF Slag, Advances in Civil Engineering, Volume 2019
9. S.C. Pala , A. Mukherjeeb , S.R. Pathakc, "Investigation of hydraulic activity of ground granulated blast furnace slag in concrete', Cement and Concrete Research 33: 1481 – 1486, 2003
10. ASTM C989, Standard Specification for Slag Cement for Use in Concrete and Mortars, American Society for Testing and Materials, West Conshohocken, PA, USA, 2014.
11. ASTM C125-13b, "Standard Terminology Relating to Concrete and Concrete Aggregates," West Conshohocken, PA: ASTM International, 2013.
12. ASTM C595, Standard Specification for Blended Hydraulic Cements, American Society for Testing and Materials, West Conshohocken, PA, USA, 2014.
13. ASTM C1157, Standard Performance Specification for Hydraulic Cement, American Society for Testing and Materials, West Conshohocken, PA, USA, 2014.
14. Young Cheol Choi, Jyoung Kim, Seongcheol Cho,"Mercury intrusion porosimetry characterization of micropore structures of high-strength cement pastes incorporating high volume ground granulated blast-furnace slag, Construction and Building Materials Vol. 37, 15 April 2017, Pages 96-103, 2017
15. Vu, T.H.; Gowripalan, N.; De Silva, P.; Paradowska, A.Z.; Garbe, U.; Kidd, P.; Sirivivatnanon, V. Assessing carbonation in one-part fly ash/slag geopolymer mortar: Change in pore characteristics using the state-of-the-art technique neutron tomography. Cem. Concr. Compos. 2020,
16. Vineet, S.; Karen, S.; Bishwajit, B.; Shashank, B. Changes in microstructure characteristics of cement paste on carbonation. Cem. Concr. Res. 2018, 109, pp. 184–197, 2018
17. Yang Song,Jun-wen Zhou,Zheng-ning Bian, and Guo-zhong Dai,"Pore Structure Characterization of Hardened Cement Paste by Multiple Methods, Advances in Materials Science and Engineering, Vol. 2019 |Article ID 3726953, 2019
18. Schiller, K.K."Porosity and Strength of Brittle Solids (with particular reference to gypsum),' in W.H, Walton (ed),'Mechanical Properties of non Metallic Materials', Butterworth, London, pp. 35-50, 1958
19. Feldman, R. F. and Beaudoin, J. J.,"Moisture and Strength of Hydrated Cement,' Cement and Concrete Research. Vol. 6 pp. 389-400, 1976
20. Xu, G., He, X. & He, Y., "Effect of Steel Slag and Granulated Blast-furnace Slag on the Mechanical Strength and Pore Structure of Cement Composites. J. Wuhan Univ. Technol.-Mat. Sci. Edit. **33,** 1186–1192, 2018
21. J. Liu and D. Wang, "Application of ground granulate blast furnace slag-steel slag composite binder in a massive concrete structure under severe sulphate attack," *Advances in Materials Science and Engineering*, vol. 2017, Article ID 9493043, 9 pages, 2017.

LIST OF FIGURES AND TABLES

Received: 29.06.2020, Revised: 12.04.2020